

In-Sensor Analytics and Energy-Aware Self-Optimization in a Wireless Sensor Node

Ningyuan Cao¹, Saad Bin Nasir¹, Shreyas Sen², and Arijit Raychowdhury¹

¹School of Electrical and Computer Engineering, Georgia Institute of Technology, Atlanta, GA

Email: nycao, saadbinnasir@gatech.edu, arijit.raychowdhury@ece.gatech.edu

²School of Electrical and Computer Engineering, Purdue University, West Lafayette, Indiana,

Email:shreyas@purdue.edu

Abstract—With the proliferation of distributed sensors and Internet of Thing end-nodes, aggregate data transfer to the back-end servers in the cloud is expected to become prohibitively large which not only results in network congestion, but also high energy expenditure at the sensor nodes. This motivates in-sensor data analytics that can perform context-aware acquisition and processing of data; and transmit data only when required. This paper presents a camera based wireless sensor node with in-sensor computation, wireless communication and end-to-end system optimization. Depending on the amount of information content and the wireless channel quality, the system chooses the minimum-energy operating-point by dynamically adjusting the processing depth (PD) and power amplifier (PA) gain. We demonstrate a complete end-to-end system and measure $3.7\times$ reduction in energy consumption compared to a baseline design where only rudimentary image compression is performed.

Index Terms—IoT, adaptive radio, self-optimizing system

I. INTRODUCTION

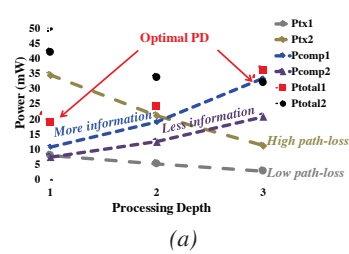
Significant growth of Internet of Things (IoT) end-nodes and high resolution of data acquisition has produced a “data deluge” in wireless sensor networks. This not only results in network congestion, degrading quality of service (QoS) in form of queueing delay, packet loss or even blocking of new connections, but also high energy expenditure and hence low battery life of energy-constrained small form-factor sensor nodes [1]. This motivates in-sensor data analysis capability in the end-node to save communication energy for the front-end devices while significantly reducing the data volume the network has to handle. However, in-sensor data analysis consumes additional energy, especially in computation-intensive applications[6]. Further, the information content as well as the environment are highly dynamic. Hence, it is desired that an intelligent system can self-optimize itself in real-time to reduce the energy consumption when deployed in unsupervised environments.

In this paper, we present a prototypical camera based wireless IoT sensor node for human detection in video surveillance applications. Depending on temporal information content and wireless channel condition, the image processing depth (PD) and power amplifier (PA) gain are dynamically adjusted in order to achieve minimum energy consumption per video frame. The principle of context-aware end-to-end energy self-optimization is illustrated in Fig. 1(a) where a high (low) path-loss results in higher (lower) communication energy necessitating more (less) in-sensor processing to maintain minimum energy dissipation. As the minimum-energy operating-point changes with both information content as well as channel quality, the system must self-optimize to determine the PD (which indicates the amount

of in-sensor analytics) as well as the PA gain on-the-fly. Here we support three processing depths (PD=1,2 or 3). Our image processing pipeline (IPP) for human detection is composed of four processing stages: object localization and segmentation through temporal difference (TD), compression (CR), feature extraction (FE) and classification (CL). One or more of these tasks can be performed at the sensor node. Each step reduces the data volume, but at the cost of computational power. PD=1 corresponds to TD and CR at the sensor node. PD=2 corresponds to TD, CR and FE; and so on (Fig. 1(b)). For $PD < 3$, the rest of the tasks of the IPP are performed at the cloud back-end. Hence, increasing PD increases computation energy/frame but reduces communication energy/frame. The overall system architecture is shown in Fig. 2. It comprises of an OV7670 camera sensor, and ADI ADSP-BF707 image processor and USRP B200 SDR (software defined radio). The implementation details including algorithm mapping, optimized use of on-board SDRAM for coefficient storage, power-gating in between frame captures and SDR programming for adaptive PA gains, are omitted here for brevity.

II. IN-SENSOR ANALYTICS

Detecting the presence of human beings plays an important role in video surveillance. The four stages of the IPP in the proposed system, namely, TD, CR, FE and CL (as described in Section I) are shown in Fig. 3. Object localization and segmentation is the pre-processing stage to detect whether a certain frame contains a moving object and segment the object for further computation or transmission. In the current implementation, we use *temporal-difference*[2] approach for pre-processing. Activated pixels will be delivered to the following processing stages if information content (S), quantified as the number of activated pixels, is larger than 3.125% ($60*40$ in a QVGA frame).



(a)

| Processing Depth (PD) | Operations |
|-----------------------|---|
| 1 | Object Segmentation+Compression |
| 2 | Object Segmentation+Compression+Feature Extraction |
| 3 | Object Segmentation+Compression+Feature Extraction+Classification |

(b)

Figure 1: (a) Power consumption changes with PD and the optimal PD for minimum-power consumption also varies under different channel conditions and information content: noisy channel and small information, thus light computation, result in more embedded processing and vice versa. (b) Operations included in each processing depth (PD).

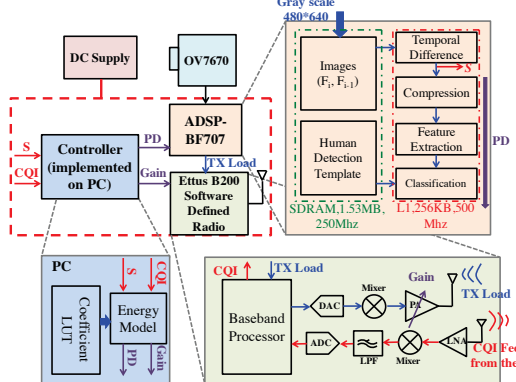


Figure 2: System architecture showing the different hardware components, the image processing pipeline (IPP) and the software defined transceiver. CQI is the channel quality index quantified by path-loss and S is the information content size defined in the following section.

Otherwise, we do not perform any further processing and the entire system is gated till the next frame is captured. The second stage of IPP is image compression. Compression reduces the data volume while maintaining a target accuracy requirement by evenly averaging over pixel windows at certain compression ratios. In our setup CR=4 is used. Feature extraction derives informative and non-redundant values to facilitate subsequent stages to generate better classification results. Among different feature descriptors, Histogram of Gradient (HOG) is chosen for its excellent performance in human recognition and large INRIA[3] human dataset availability for training and testing. HOG generates histogram of orientations for each block in the image. Classification is the final step in the IPP. The classifier is trained offline in testing phase and classification template is generated and stored in the SDRAM as shown in Fig. 2. In our implementation, Naive Bayes (NB) classifier [4] is applied. An average of 87% detection accuracy is achieved by applying NB classifier on extracted HOG features.

With “deeper” processing (increasing PD) along the IPP, transmission data volume decreases significantly at the expense of higher computation energy as is shown in Fig. 4a. Fig. 4b shows a clear trade-off between communication and computation of in-sensor data analytics of the proposed system.

III. ADAPTIVE WIRELESS COMMUNICATION

Wireless communication, conventionally is the major source of energy expenditure and shortened battery-lifetime of wireless sensors. To implement energy-efficient wireless transceiver on SDR (software defined radio), the performance/energy characteristics of the USRP B200 SDR is first explored. Fig. 5a plots

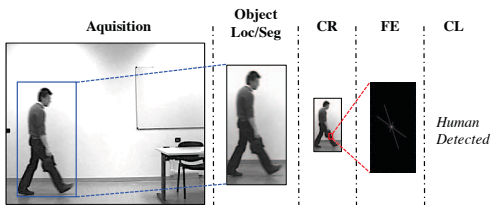


Figure 3: Algorithm demonstration with a real video frame. The system first locates and segments moving object from captured raw image and further compresses the segmented sub-image; then the feature descriptor will be extracted from the compressed object in feature extraction stage (FE) and fed to the template in the last stage for final classification (CL).

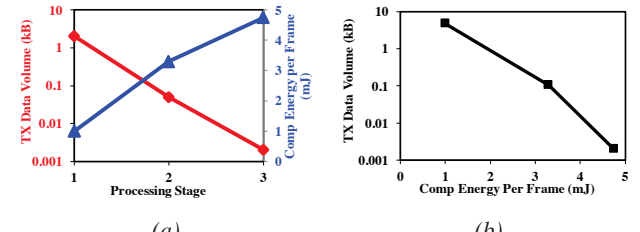


Figure 4: (a) Measured transmission data volume and computation energy vs processing depth. (b) Estimated transmission data volume vs. computation energy.

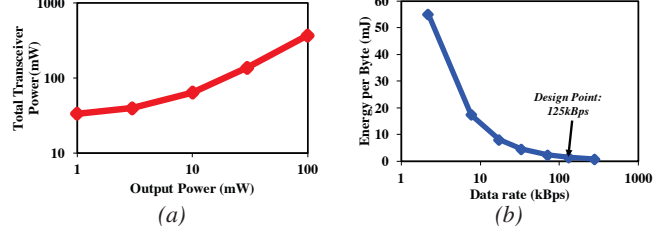


Figure 5: Measured (a) transceiver power vs. output power. (b) energy per byte vs. data rate.

the total measured transceiver power, as a function of output power. For low output power, the system is limited by the bias/standby/fixed power while the total power increased proportionately when output power is high. In Fig. 5b, it is observed that with the increase of data rate, energy per byte decreases. In our system, data rate is set at 125kBps by GNUradio.

Non-adaptive IoT communication links are designed for the worst-case, i.e., the maximum output power (100mW as is shown in the measured results of Fig. 5a) to guarantee target bit-error-rate (BER) under the worst case channel conditions. However, as channel condition varies significantly particularly for mobile nodes, adaptive wireless communication is desired [5,8,9,10,11]. It adjusts the transceiver gain (power) dynamically to operate at power back-off modes depending on the channel quality. The channel quality is affected by path-loss which results in the signal strength attenuation and increased BER. Path-loss in dB is expressed as [7]:

$$\text{Path_loss} = 20\log_{10}\left(\frac{4\pi d f}{c}\right) \quad (1)$$

Here d is distance, f is the carrier frequency and c is the speed of light. In our design, the carrier frequency is 985Mhz. To compensate for path-loss, the PA gain is adjusted dynamically to guarantee minimum BER. Measured BER vs. path-loss for different PA gains of the SDR are shown in Fig. 6a. The PA gain and the total transmission power required to meet a target $\text{BER}=10^{-8}$ for different path-loss are also shown in Fig. 6b. We intentionally choose a conservative target BER. For lower

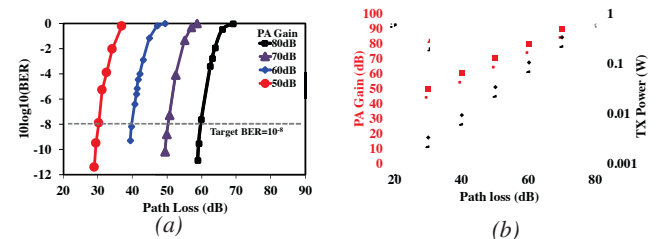


Figure 6: Measured (a) bit-error-rate vs. channel path loss with different PA gain. (b) PA gain and transceiver power vs. path loss for adaptive radio at target $\text{BER}=10^{-8}$.

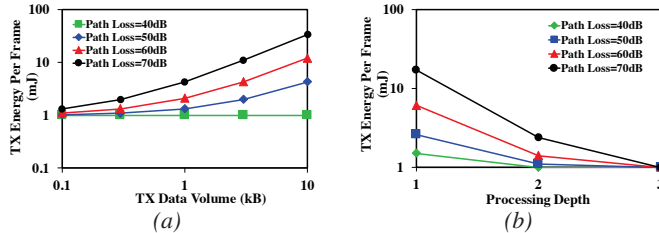


Figure 7: Measured (a) transmission energy per frame vs transmission data volume under various channel conditions. (b) Transmission energy per frame vs. processing depth under different path-loss conditions.

BER targets, communication power decreases and the importance of in-sensor processing is even higher making the proposed self-optimizing scheme even more relevant. We measure the total transmitted energy as a function of the total transmitted data volume. For low path loss, the standby power dominates, however with increasing path loss and PA gain we see a near-linear increase in total transmission energy as a function of the data volume (Fig. 7a). Since, the volume of transmitted data decreases with PD, we can now estimate the total transmission energy per frame of video data as a function of PD, as shown in Fig. 7b. With clean channel (40dB path-loss), transmission energy per frame is 1mJ for transmission after PD1, while for noisy channel (70dB path-loss), transmission energy per frame can be as high as 17mJ.

IV. REAL-TIME CONTEXT-AWARE SELF-OPTIMIZATION

We first develop a model for the total energy of the sensor node. The total energy, E , includes computation energy, E_p , and communication energy, E_{TX} . E_p increases linearly with information content S and E_{TX} depends on transmission data volume (a function of S and PD) as well as dynamic transmission power (a function of path-loss). DR is the data rate of transmission.

$$E_p = \theta_{PD}S + E_{\text{static},p} \quad (2)$$

$$E_{TX} = P_{\text{dynamic,TX}}(PL) \cdot \frac{\Gamma(S, PD)}{DR} + E_{\text{static,TX}} \quad (3)$$

Here θ and Γ are model parameters which are fitted via regression during pre-deployment testing and calibration. During test/calibration, these model coefficients are generated for different information content, processing depth and path-loss by exciting random operating conditions. Finally we use regression for model fitting and store the result in a look up table (LUT). LUT values are used during run-time self-optimization, which is performed every 1s. After deployment, information about path-loss is sent from back-end cloud as channel quality information (CQI) data (Fig. 2) to the sensor node periodically and the minimum PA gain needed to compensate for path-loss is updated. Then the energy model estimates the energy for all the IPP blocks with respect to the information content. Finally, the system chooses the PD for minimum energy of operation. PD, PA gain and data size are packed into the frame header and transmitted along with the video data (dependent on the PD). This is used by cloud server for back-end processing. The calibration and run-time self-optimization scheme are shown in Fig. 8.

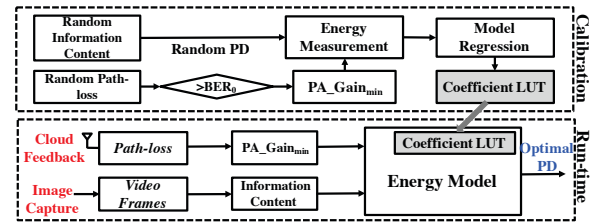


Figure 8: Flow-chart illustrating test/calibration and run-time self-optimizing.

V. END-TO-END SYSTEM MEASUREMENTS

Based on the model parameters obtained during calibration, the system chooses the operating mode for minimum energy per frame depending on S and PL. This is shown in Fig. 9a. As the PL changes, the proposed platform always selects the PD with minimum overall energy. The corresponding PA gain is also adjusted to maintain BER for the given PL. A trend of “deeper” processing along with worse channel quality is measured. A peak saving of $3.7\times$ at 70dB path-loss is measured when compared with a baseline design where only object localization and compression are performed and then the compressed data is transmitted. We tested in various indoor and outdoor settings with varying PL and S; and we provide measurements for a sample set. We compare our system with two competing static designs (1) Tx-All design where no in-sensor analytics is performed and all the data is transmitted with channel-adaptive PA gain and (2) Full-Computation design where the entire IPP pipeline is implemented independent of the channel condition or information content. We observe that the proposed self-optimizing system always tracks the minimum energy-point by choosing the correct PD (Fig. 9b). A dynamic channel is shown by moving the mobile sensor node while keeping the base station static. We measure key system parameters and observe how the overall system self-optimizes in run-time to minimize energy consumption (Fig. 10).

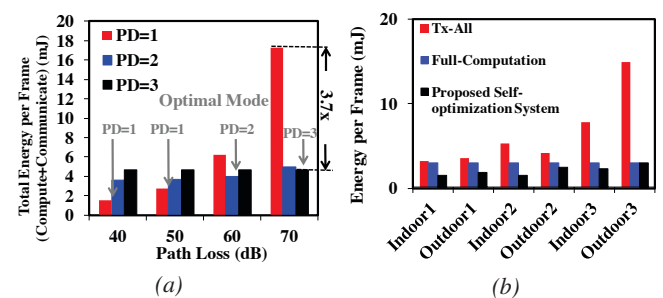


Figure 9: (a) Measured total energy per frame under different path-loss conditions and processing depth. The optimal processing depth is denoted in the figure. (b) Average energy consumption per frame under various environments using different strategies.

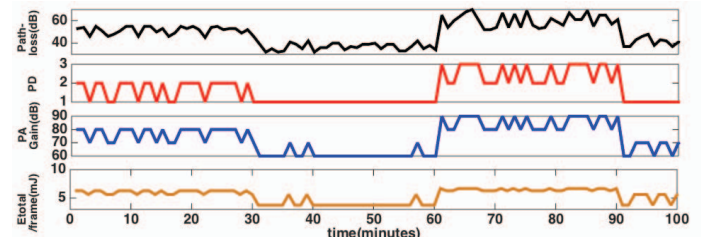


Figure 10: Case study for mobile sensor node with varying path-loss and correspondingly self-optimizing PD, PA gain, and total energy/frame.

VI. CONCLUSIONS

This paper presents a camera based wireless IoT sensor node which self-optimizes itself between the computation and the communication. As the information content and the channel conditions change, the system tracks the minimum energy point. Hardware measurements show $3.7\times$ reduction of the total energy/frame compared to a baseline design.

ACKNOWLEDGMENT

This work was sponsored by the Semiconductor Research Corporation under Grant no. 2720.001.

REFERENCES

- [1] J. Yick, B. Mukherjee, and D. Ghosal, "Wireless sensor network survey," *Computer Networks*, vol. 52, no. 12, pp. 2292–2330, Aug. 2008.
- [2] K. Kinoshita, M. Enokidani, M. Izumida, and K. Murakami, "FPGA implementation of moving object detection in frames by using background subtraction algorithm," in *Robotics and Vision 2006 9th International Conference on Control, Automation, 2006*, pp. 1–6.
- [3] N. Dalal and B. Triggs, "Histograms of oriented gradients for human detection," in *2005 IEEE Computer Society Conference on Computer Vision and Pattern Recognition (CVPR'05)*, 2005, vol. 1, pp. 886–893 vol. 1.
- [4] S. McCann and D. G. Lowe, "Local Naive Bayes Nearest Neighbor for image classification," in *2012 IEEE Conference on Computer Vision and Pattern Recognition*, 2012, pp. 3650–3656.
- [5] D. Banerjee, S. Sen, and A. Chatterjee, "Self learning analog/mixed-signal/RF systems: Dynamic adaptation to workload and environmental uncertainties," in *2015 IEEE/ACM International Conference on Computer-Aided Design (ICCAD)*, 2015, pp. 59–64.
- [6] A. Anvesha, S. Xu, N. Cao, J. Romberg, and A. Raychowdhury, "A Light-powered, 'Always-On', Smart Camera with Compressed Domain Gesture Detection," in *Proceedings of the 2016 International Symposium on Low Power Electronics and Design*, New York, NY, USA, 2016, pp. 118–123.
- [7] S. Y. Seidel and T. S. Rappaport, "914 MHz path loss prediction models for indoor wireless communications in multifloored buildings," *IEEE Transactions on Antennas and Propagation*, vol. 40, no. 2, pp. 207–217, Feb. 1992.
- [8] S. Sen, et.al., "Environment-Adaptive Concurrent Companding and Bias Control for Efficient Power-Amplifier Operation," *IEEE Transactions on Circuits and Systems I: Regular Papers*, vol. 58, no. 3, pp. 607–618, Mar. 2011.
- [9] S. Sen, et.al., "A Power-Scalable Channel-Adaptive Wireless Receiver Based on Built-In Orthogonally Tunable LNA," *IEEE Transactions on Circuits and Systems I: Regular Papers*, vol. 59, no. 5, pp. 946–957, May 2012.
- [10] S. Sen, V. Natarajan, S. Devarakond, and A. Chatterjee, "Process-Variation Tolerant Channel-Adaptive Virtually Zero-Margin Low-Power Wireless Receiver Systems," *IEEE Transactions on Computer-Aided Design of Integrated Circuits and Systems*, vol. 33, no. 12, pp. 1764–1777, Dec. 2014.
- [11] S. Sen, V. Natarajan, R. Senguttuvan, and A. Chatterjee, "PROVIZOR: Process tunable virtually zero margin low power adaptive RF for wireless systems," in *2008 45th ACM/IEEE Design Automation Conference*, 2008, pp. 492–497.